

increasing part of our model, and so the maximal x-ray flux is not yet reached after 2 days. Expressed in physical units, the shell velocity depends on the mass loss rate, \dot{M} , the wind velocity, v_{wind} , in the x-ray-emitting region, and the energy-dependent absorption coefficient, σ , of the absorbing wind material.

For $r_{\tau=1}/R_* = 7.5$, which is the mean radius of optical depth unity for the wind properties of ζ Orionis (8) in the energy range of 0.6 to 1.0 keV, where the enhanced x-ray emission appeared during the first 2 days, we derive a best-fit shell velocity of 570 km/s. From the analytical velocity field $v(r) = v_\infty(1 - R_*/r)^\beta$, which describes the velocity of the smooth wind in an O-type star, we determine a wind velocity of 1600 km/s in the vicinity of the shell after 2 days. Therefore, in the star's frame the post-shock gas moves outward but more slowly than the ambient wind (reverse shock). Using again 1600 km/s (in the star frame) as the characteristic speed of unshocked wind material entering the shock, we deduce a shock velocity of ≈ 1000 km/s (in the star frame), which is consistent with the temperature of the x-ray-emitting material derived from a spectral fit of our PSPC data, given the errors of the deduced shock velocity.

We emphasize that a model of a shell propagating with the velocity of the ambient wind (thin dotted line in Fig. 2) cannot fit the observed increase in x-ray count rate. Such a model would lead to an increase and a disappearance of the shell's x-ray emission that are much faster than those observed. With our model of a propagating shock in the wind, we can explain the observed increase in x-ray count rate observed for ζ Orionis. The result of our calculations for the flow of the post-shock gas in the stellar wind of ζ Orionis confirms the results of the wind models that predict that reverse shocks in stellar winds are much stronger than forward shocks. Our ROSAT observations of ζ Orionis provide the first direct observational evidence for the existence of propagating shock waves in the winds of hot stars.

REFERENCES AND NOTES

1. T. Chlebowski, F. R. Hamden Jr., S. Sciortino, *Astrophys. J.* **341**, 427 (1989).
2. T. W. Berghöfer and J. H. M. M. Schmitt, in *Proceedings of the International Astrophysical Union Symposium 162 on Pulsation, Rotation and Mass Loss in Early-Type Stars*, L. Balona et al., Eds. (Kluwer, Dordrecht, the Netherlands, 1993).
3. K. S. Long and R. L. White, *Astrophys. J.* **239**, L65 (1980).
4. J. P. Cassinelli and G. L. Olson, *ibid.* **229**, 304 (1979).
5. W. L. Waldron, *ibid.* **282**, 256 (1984).
6. D. Baade and L. B. Lucy, *Astron. Astrophys.* **178**, 213 (1987).
7. J. P. Cassinelli and J. H. Swank, *Astrophys. J.* **271**, 681 (1983).
8. T. W. Berghöfer and J. H. M. M. Schmitt, *Astron. Astrophys.*, in press.
9. L. B. Lucy and P. M. Solomon, *Astrophys. J.* **159**, 879 (1970).
10. J. L. Castor, D. C. Abbott, R. I. Klein, *ibid.* **195**, 157 (1975).
11. K. B. MacGregor, L. Hartmann, J. C. Raymond, *ibid.* **231**, 514 (1979).
12. L. B. Lucy and R. L. White, *ibid.* **241**, 300 (1980).
13. S. P. Owocki, J. I. Castor, G. B. Rybicki, *ibid.* **335**, 914 (1988).
14. D. J. Hillier et al., *Astron. Astrophys.* **276**, 117 (1993).
15. J. Trümper, *Adv. Space Res.* **2** (4), 241 (1983).
16. J. Trümper et al., *Nature* **349**, 579 (1991).
17. E. Pfeiffermann et al., *Soc. Photoopt. Instrum. Eng.* **733**, 519 (1986).
18. The ROSAT project has been supported by the Bundesministerium für Forschung und Technologie (BMFT) and the Max-Planck-Gesellschaft (MPG). We acknowledge the support of our colleagues from the ROSAT group and thank A. Feldmeier for a copy of his doctoral thesis, which has given us useful information and inspiration for the interpretation of the presented x-ray data.

2 May 1994; accepted 29 July 1994

Stabilization of Atomic Hydrogen in Both Solution and Crystal at Room Temperature

Riichi Sasamori, Yoshihiro Okaue, Toshiyuki Isobe, Yoshihisa Matsuda*

Atomic hydrogen has been stably encapsulated in both solution and crystal at room temperature. Upon γ -ray irradiation of $[(\text{CH}_3)_3\text{Si}]_8\text{Si}_8\text{O}_{20}$, which is the trimethylsilylated derivative of the silicate anion with a double four-ring (D4R) cage, electron spin resonance (ESR) spectra revealed that a single hydrogen atom is encapsulated in the center of the D4R cage and is stable for periods of many months. Attack by chemically reactive species such as oxygen was prevented by the D4R cage, but the ESR signal of the hydrogen atom was sensitive to the magnetic interaction caused by the presence of the O_2 molecule near the cage.

The hydrogen atom, the simplest of atoms and free radicals, is difficult to trap at ambient temperature because of its high activity and small size. Electron spin resonance has been used to study hydrogen atoms in several matrices, including KCl, CaF_2 , quartz, rare gas ices, and acid ices (1). In these matrices, the ESR signals of atomic hydrogen were observed only at low temperatures such as 4.2 and 77 K because the trapped hydrogen was unstable. In some cases, after the matrix was warmed to room temperature for a few minutes and cooled again, the signal disappeared (2). On the other hand, there is an example of an x-ray-irradiated human tooth in which atomic hydrogen is stabilized at room temperature in an inorganic medium (3). However, the above hydrogen radical centers have not been made in a compound with a cage structure, which can encapsulate a single hydrogen atom and protect it against the reactive surroundings. In our study, we succeeded in stably trapping atomic hydrogen at room temperature upon γ -ray irradiation of $[(\text{CH}_3)_3\text{Si}]_8\text{Si}_8\text{O}_{20}$, which is the trimethylsilylated derivative of silicate anion with a D4R structure. The ESR spectra revealed that atomic hydrogen was present. This hydrogen atom is most likely encapsulated in the center of the D4R framework structure in both solution and crystal for a long time.

The above compound was synthesized by

trimethylsilylation of tetramethylammonium silicate, $[(\text{CH}_3)_4\text{N}]_8\text{Si}_8\text{O}_{20} \cdot \text{XH}_2\text{O}$ (4). The crystals obtained were analyzed by infrared spectroscopy, elemental analysis, and gas chromatography. The single-crystal x-ray structure analysis, which was performed at room temperature, revealed that the molecule crystallized in the space group $P\bar{1}$ with one equivalent molecule in the unit cell (observed density, D_{O} , of 1.181 g cm^{-3}). Although the R values, as expected, did not become smaller because of the large temperature factors of the terminal methyl group (5), the core structure of the $[(\text{CH}_3)_3\text{Si}]_8\text{Si}_8\text{O}_{20}$ could be determined. Figure 1 illustrates the cube-like structure with a cavity at a center in the D4R framework. The average packing distances for neighboring and diagonal Si-Si atoms in the D4R framework are 3.079 ± 0.004 , 4.355 ± 0.004 , and $5.329 \pm 0.007 \text{ \AA}$, respectively. Similarly, the O-O packing distances are 2.607 ± 0.009 , 3.687 ± 0.008 , and $5.197 \pm 0.013 \text{ \AA}$, respectively. A space-filling representation of the structure made by use of the van der Waals radii of silicon and oxygen reveals that a cavity in the D4R cage can encapsulate a hydrogen atom and that the meshes of the D4R cage are much smaller than that of a hydrogen atom.

An ESR spectrum of atomic hydrogen encapsulated in polycrystalline $[(\text{CH}_3)_3\text{Si}]_8\text{Si}_8\text{O}_{20}$ by irradiation with ^{60}Co γ -rays [10^5 Grays (Gy)] at room temperature is given in Fig. 2A. The ESR spectral feature is similar to that of irradiated quartz at 77 K (2). Two

Department of Chemistry, Faculty of Science, Kyushu University, Higashi-ku, Fukuoka, 812 Japan.

*To whom correspondence should be addressed.

sharp, hyperfine lines due to atomic hydrogen are separated by 50.804 mT accompanied with two weak satellite lines, respectively. The satellite lines are attributable to super hyperfine splitting on the basis of ^{29}Si with a nuclear spin, I , of $1/2$ and a natural abundance of 4.67%. There is another possibility for the origin of the satellite lines. The dipole-dipole coupling of the trapped hydrogen with protons of peripheral methyl groups can cause the satellite lines (spin-flip satellite lines) to arise (6). The satellite lines were possibly caused by both hyper-fine and dipole-dipole interactions. The Zeeman splitting factor (g value) and hyperfine splitting constants, A , were obtained from the strict calculations (7) of $g = 2.0022$ and $A = 1415.3$ MHz. There is only a small difference in the parameters from the free-atom values ($g = 2.002256$ and $A = 1420.40573$ MHz) (8), perhaps due to van der Waals effects. The spin density was 4.3×10^{-5} spins per $[(\text{CH}_3)_3\text{Si}]_8\text{Si}_8\text{O}_{20}$ unit. The angular dependence of ESR spectra for a single crystal revealed that the g value and the hyperfine coupling constant are isotropic. These signals can be observed at room temperature even after 2 years from the time of irradiation. Therefore, the size of the cavity in the D4R cage is suitable for the hydrogen atom, and the degree of chemical effect from the outside through meshes of the

D4R cage is negligible. Furthermore, the above compound with a D4R cage is soluble in some solvents. Consequently, it is possible to prepare a solution, polycrystal and single-crystal, that includes the single hydrogen atom. In fact, even in a dichloromethane or diethyl ether solution of an irradiated specimen, the ESR signals of atomic hydrogen can be observed at room temperature for a period longer than 1 year (Fig. 2B). To our surprise, the polycrystal obtained again from the above solution showed the ESR signals of atomic hydrogen at room temperature. No ESR signal caused by the hydrogen was detected for a D3R cage with a smaller cage size than the D4R cage. We concluded that a single atomic hydrogen is fitted in size and stably encapsulated at a center in the D4R cage structure at room temperature in both solution and solid.

The ESR spectrum was reproducible upon iterative cooling and warming in the range of room temperature to 77 K. The atomic hydrogen exists stably in the low-temperature range. At the high-temperature range, atomic hydrogen remains until 100°C . However, after heating up to 150°C , the ESR signals disappeared and did not reappear upon cooling to room temperature. Atomic hydrogen probably escapes from the D4R silicate cage at high temperatures.

The pressure dependence of the ESR

signal intensities of atomic hydrogen was measured in the pressure range of 2 Pa to atmospheric pressure at room temperature (Fig. 3). There was little variation in signal intensities under high vacuum, indicating that atomic hydrogen does not come out of the D4R cage and stably exists even under the high vacuum. Measurements of ESR were also carried out under these pressures of air, oxygen, or nitrogen. The pressure dependencies of the apparent ESR signal intensities under the atmospheres of air, oxygen, or nitrogen with constant microwave power are shown in Fig. 3. The signal intensities under the nitrogen atmosphere were constant independently of the degree of vacuum. However, the signal was reduced in its apparent intensity upon evacuations under both the air and oxygen atmospheres. The signal intensities under the oxygen atmosphere were several times as strong as those under the air at the range of 3×10^3 to 1×10^5 Pa. This reduction in apparent intensity was due to saturation in microwave power because of the increase in the spin-lattice relaxation time, T_1 . The signal intensities were in-

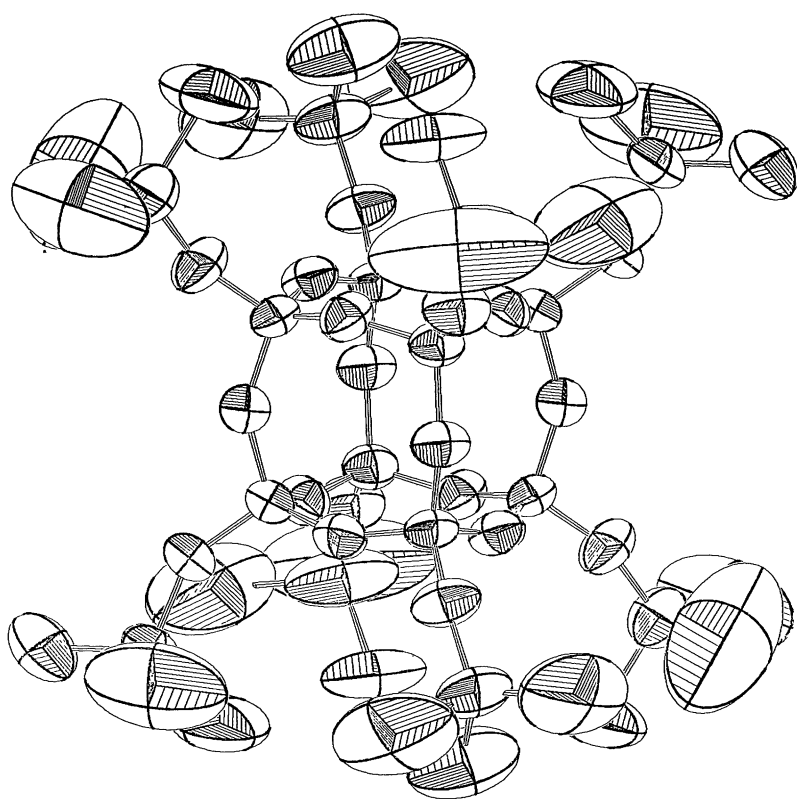


Fig. 1. Structure of the $[(\text{CH}_3)_3\text{Si}]_8\text{Si}_8\text{O}_{20}$.

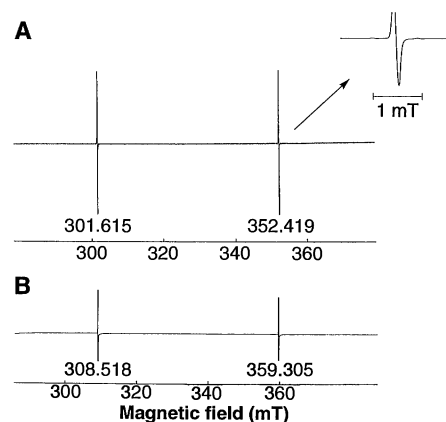


Fig. 2. (A) ESR spectrum of atomic hydrogen in γ -irradiated polycrystalline $[(\text{CH}_3)_3\text{Si}]_8\text{Si}_8\text{O}_{20}$ at room temperature (microwave frequency, ν , of 9.2185 GHz). (B) ESR spectrum for diethyl ether solution of γ -irradiated specimen ($\nu = 9.4128$ GHz).

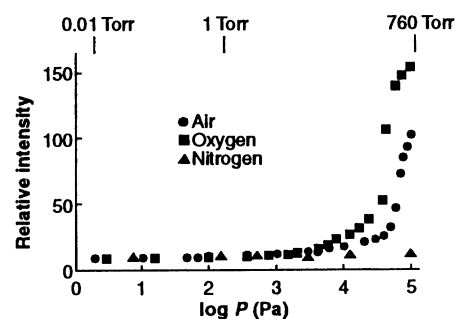


Fig. 3. Effects of pressures of air, oxygen, and nitrogen on apparent signal intensities.

fluenced by paramagnetic oxygen gas, and the hydrogen atom was stable with respect to the oxygen molecules near the D4R cage. The fluctuation of the local magnetic field at the encapsulated atomic hydrogen is induced by triplet oxygen and affects spin-lattice relaxation. The saturation power depended on the O₂ pressure in a manner quite similar to the way the apparent intensity does. These observations show clearly that the hydrogen atom is encapsulated in the D4R cage and can experience the magnetic field induced by O₂ molecules outside the cage without chemical attack by the latter. The D4R cage in the crystalline state has free space around itself. In that space, oxygen molecules can reach near the cage. The free space is maintained by bulky trimethylsilyl groups.

Relaxation times were determined by electron spin echo (ESE) for the main lines that are split only by the hydrogen nucleus. Echo signals were not obtained at room temperature because of their fairly small relaxation times, so the measurement was performed for the degassed sample at 77 K. From two-pulse and three-pulse ESE decays of the atomic hydrogen sample (Fig. 4), the phase memory time, t_M , of 0.87 μ s and the spin-lattice relaxation time, t_1 , of 13 μ s were obtained. Thus, the phase memory time is considered to be constant because the line shape of the ESR signal was invariable with respect to temper-

ature, degree of vacuum, and exposure gas. The spin-lattice relaxation time likely has a relatively large temperature dependence, because echo signals were not obtained at room temperature. This temperature dependence probably arises from the motion of the terminal methyl group and, accordingly, corresponds to the large ellipsoids for methyl carbon in the crystal structure analysis.

We could not encapsulate hydrogen atoms in D3R silicate cages as mentioned earlier and we have yet to study the larger D5R, D6R, and D7R silicate cages (9). These cages provide a chemically shielded space in which an atom or atoms can behave just as in the free state. The construction of new cages should lead to novel developments in the study of atoms and atom-cluster interactions.

REFERENCES

1. G. E. Pake and T. L. Estle, *The Physical Principles of Electron Paramagnetic Resonance* (Benjamin, Reading, MA, ed. 2, 1973), pp. 233–240.
2. R. A. Weeks and M. Abraham, *J. Chem. Phys.* **42**, 68 (1965).
3. T. Cole and A. H. Silver, *Nature* **200**, 700 (1963).
4. D. Hoebbel and W. Wieker, *Z. Anorg. Allg. Chem.* **384**, 43 (1971).
5. Yu. I. Smolin, *ACS Symp. Ser.* **194**, 329 (1982).
6. G. T. Trammell, H. Zeldes, R. Livingston, *Phys. Rev.* **110**, 630 (1958); M. Bowman, L. Kevan, R. N. Schwartz, *Chem. Phys. Lett.* **30**, 208 (1975); B. L. Bales and E. S. Lesin, *J. Chem. Phys.* **65**, 1299 (1976).
7. J. E. Wertz and J. R. Bolton, *Electron Spin Resonance: Elementary Theory and Applications* (McGraw-Hill, New York, 1972), pp. 434–445.
8. S. N. Foner, E. L. Cochran, V. A. Bowers, C. K. Jen, *J. Chem. Phys.* **32**, 963 (1960).
9. P. A. Agaskar, V. W. Day, W. G. Klemperer, *J. Am. Chem. Soc.* **109**, 5554 (1987).

22 March 1994; accepted 29 July 1994

Stern-Volmer in Reverse: 2:1 Stoichiometry of the Cytochrome c–Cytochrome c Peroxidase Electron-Transfer Complex

Jian S. Zhou and Brian M. Hoffman*

A reverse protocol for measurements of molecular binding and reactivity by excited-state quenching has been developed in which the quencher, held at a fixed concentration, is titrated by a photoexcitable probe molecule whose decay is monitored. The binding stoichiometries, affinities, and reactivities of the electron-transfer complexes between cytochrome c (Cc) and cytochrome c peroxidase (CcP) were determined over a wide range of ionic strengths (4.5 to 118 millimolar) by the study of photoinduced electron-transfer quenching of the triplet excited state of zinc-substituted Cc (ZnCc) by Fe³⁺CcP. The 2:1 stoichiometry seen for the binding of Cc to CcP at low ionic strength persists at the physiologically relevant ionic strengths and likely has functional significance. Analysis of the stoichiometric binding and rate constants confirms that one surface domain of CcP binds Cc with a high affinity but with poor electron-transfer quenching of triplet-state ZnCc, whereas a second binds weakly but with a high rate of electron-transfer quenching.

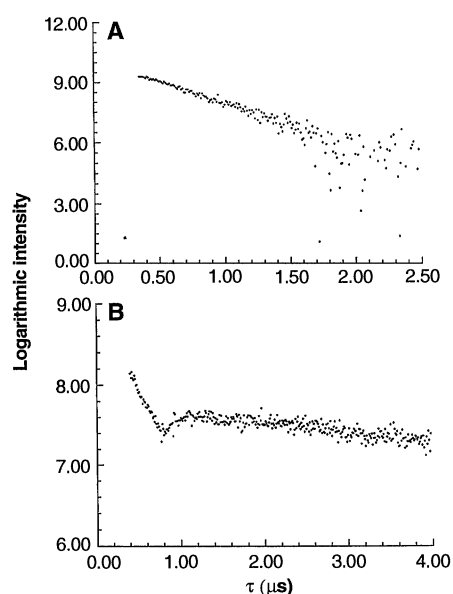


Fig. 4. Envelopes against the interval between the first and second pulses, τ , of (A) two-pulse spin echo and (B) three-pulse spin echo for atomic hydrogen in γ -irradiated $[(\text{CH}_3)_3\text{Si}]_8\text{Si}_8\text{O}_{20}$ at 77 K. Conditions: (A) $\nu = 8.952155$ GHz, magnetic field (H) = 342.733 mT, pulse width = 40 ns; (B) $\nu = 8.95167$ GHz, $H = 342.711$ mT, pulse width = 40 ns, interval between the second and third pulses (τ) = 400 ns.

Measurements of excited-state quenching have been important for no less than the 75 years since the original Stern-Volmer report (1) and have been used to study the binding of one biomolecule to another for nearly half a century (2–6). In particular, recent quenching studies of protein-protein electron-transfer complexes, which are representative of even more complicated assemblies in photosynthesis and respiration, give information about binding (7, 8) and interfacial dynamics and recognition (9–12) as well as the electron-transfer process itself (13, 14). Despite the wide use of quenching methods, the basic experiment has remained unchanged: A probe molecule at

fixed concentration is examined while being titrated with the quencher. Even our recent study (8), which showed that CcP can bind two molecules of Cc under low-salt conditions, although unusual in that it involved a titration of a “substrate,” Cc, with an enzyme, CcP, used this basic procedure. Here we describe a “reverse” quenching experiment: The quencher at fixed concentration is titrated by the probe molecule. Through the use of this protocol, we demonstrate that the 2:1 stoichiometry seen for the binding of Cc to CcP at low ionic strength persists at the physiologically relevant ionic strengths and thus is likely to have functional significance. The results further provide the means for analyzing the dependence of the electron-transfer rate constant on ionic strength in terms of changes in the distribution among multiple structures of a complex.

Department of Chemistry, Northwestern University, Evanston, IL 60208–3113, USA.

*To whom correspondence should be addressed.